

Example 1 is calculated based on a typical IGBT pulse frequency of 10 kHz. The result shows that there is no deviation between the average and maximum values of the junction temperature due to the low thermal impedances at high frequencies.

The pulse frequency in example 2 and 3 had been reduced to 2 kHz, however keeping constant values for the amount of energy dissipation in example 2 and for the average and maximum total power dissipation in example 3. Both examples show a deviation between average and maximum junction temperature.

Simply expressed, it may be presumed that a calculation based on average power dissipation and static thermal resistance is sufficient for pulse frequencies above about 3 kHz.

Example 4 shows the drastic difference between average and maximum junction temperature at very low pulse frequencies.

3.2.2.4 Junction temperature at fundamental harmonics frequency

Calculation of the junction temperature determined by the fundamental frequency of the converter output current is only efficient, when it is computer-aided.

The thermal system as well as the electrical system per pulse duration have to be calculated in detail in order to integrate the IGBT and diode junction temperature over a sine half-wave.

Figure 3.12 shows a principal calculation scheme which had been elaborated in source [194].

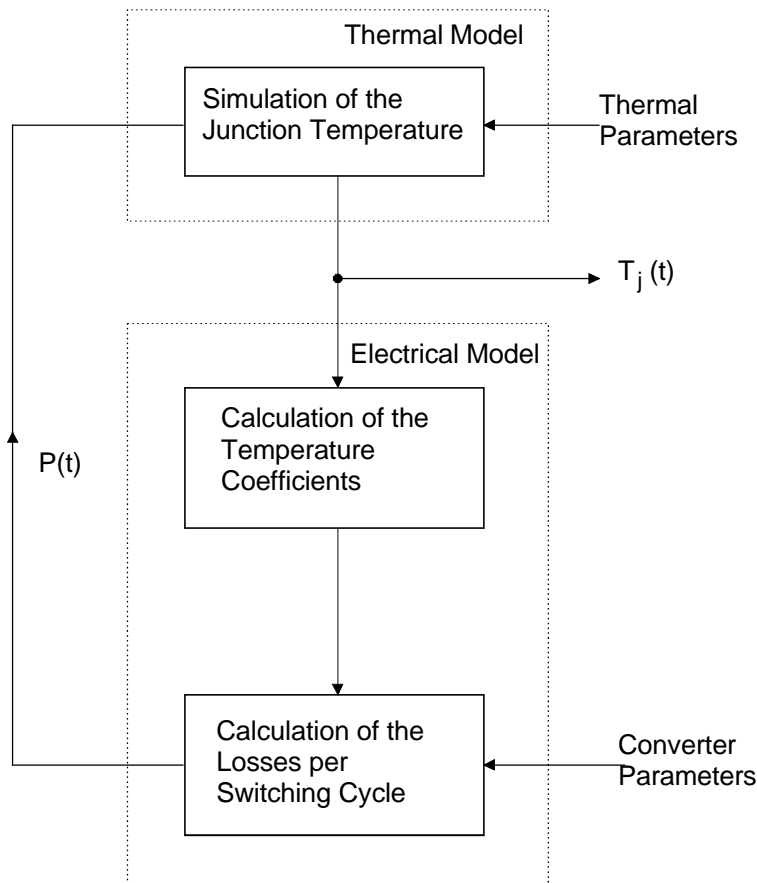


Figure 3.12 Principal calculation of the junction temperature in converters with sinusoidal output currents [194]

The thermal model mainly corresponds to Figure 3.8 simulating the thermal impedances by means of RC-elements.

Switching losses per pulse may be calculated based on stored characteristics, if the current converter parameters such as DC-link voltage and instantaneous load current are given. The

instantaneous junction temperature is entered into the calculation via the temperature coefficients.

Figure 3.13 shows the power dissipation time characteristic and the average power dissipation in an IGBT as well as the resulting junction temperature characteristics for different basic output frequencies as the result of a simulation according to [194].

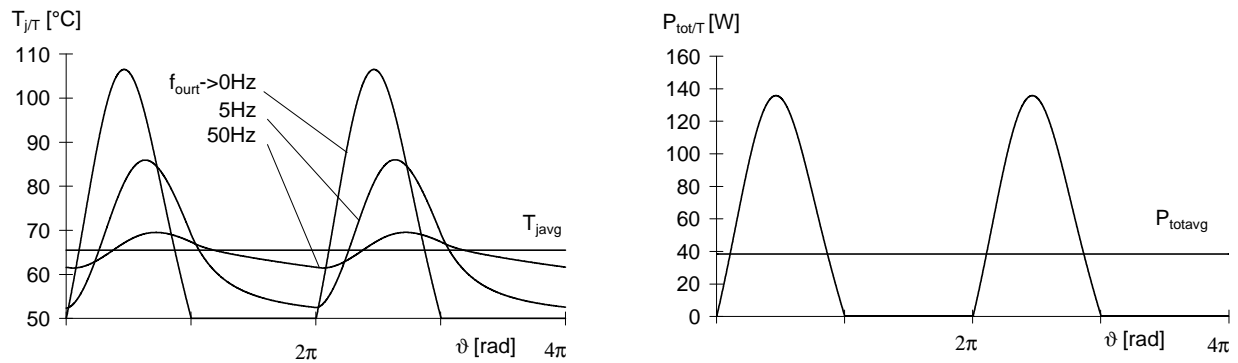


Figure 3.13 Simulated junction temperature and power dissipation characteristics of a 1200V/50A-IGBT under inverter operation for different fundamental output frequencies; [194]

$$V_d = 540 \text{ V}; i_{1\text{RMS}} = 25 \text{ A}, f_s = 8 \text{ kHz}; \cos \varphi = 0.8; m = 0.8; T_h = 50^\circ\text{C}$$

In this example, the maximum junction temperature exceeds the average value by just about 4-5 K at a frequency of 50 Hz.

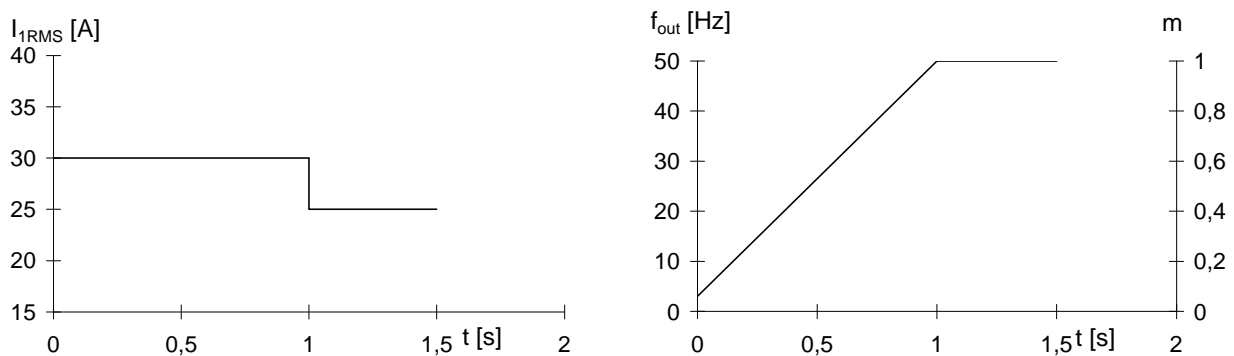
For low frequencies the average junction temperature is no longer permitted to determine the thermal layout of the system because of its clearly increased maximum value.

Consequently, the permissible output current RMS-Value for a defined power module will decrease at a given heatsink temperature and switching frequency.

Corresponding performance characteristics (e.g. for SKiiPPACK) are available by SEMIKRON on request.

Moreover, Figure 3.13 shows that no temperature ripples with high pulse frequency arise. This is also confirmed by the calculations in chapter 3.2.2.3.

A very particular special case with regards to the thermal stress of power modules is the voltage- and frequency-controlled starting procedure of a three-phase motor drive supplied by an inverter. Figure 3.14 shows a related simulation example.



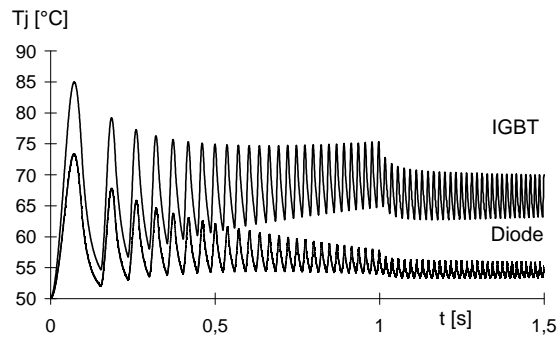


Figure 3.14 Start-up of a three-phase motor drive (parameters as in Figure 3.13), [194]

3.2.3 Evaluation of temperature characteristics with regards to module life

Power dissipation alterations below a repetition frequency of about 3 kHz will not be smoothed by the transient thermal impedance of the chips any longer and will lead to temperature fluctuations in the module (see chapter 3.2.2).

As already mentioned in chapter 1.4.2.4, all internal connections of power modules are subject to wear and tear caused by temperature fluctuations. This fatigue of material is caused by thermal stress due to the different expansion coefficients of the connected materials.

Therefore, it is important for thermal dimensioning to check, whether the chip temperature fluctuations generated during periodic power cycling (pulse frequency, fundamental frequency, power cycle) are so intensive that, in the worst case, the required number of cycles may not be reached. In this case, not the maximum chip temperature T_{jmax} , but the temperature difference $\Delta T_j = T_{jmax} - T_{jmin}$ during given power cycles is considered as limit value for power losses of the module.

The correlation between the possible number of power cycles n and the temperature cycling amplitude ΔT_j is subject to the influence of many parameters. Corresponding measurements require a lot of time and effort, see chapter 2.7 and [231].

In tests with active power cycles the lifetime of a power module depends not only on the temperature difference ΔT_j but also on the average (medium) temperature T_m in the test procedure. This was confirmed clearly by the results of LESIT-research project [303].

LESIT results of power cycling lifetime tests with power modules by different manufacturers are shown in Figure 3.15. The parameter adjustment was done by SEMIKRON. These results represent the state-of-the-art in 1995. Meanwhile, the lifetime was increased by improved solder connections and optimized wire bond connections. So, 20000 cycles at $\Delta T=100^\circ\text{C}$ and $T_{j,min}=40^\circ\text{C}$ are achieved. Presently, updated characteristics for SEMIKRON power modules are in preparation.

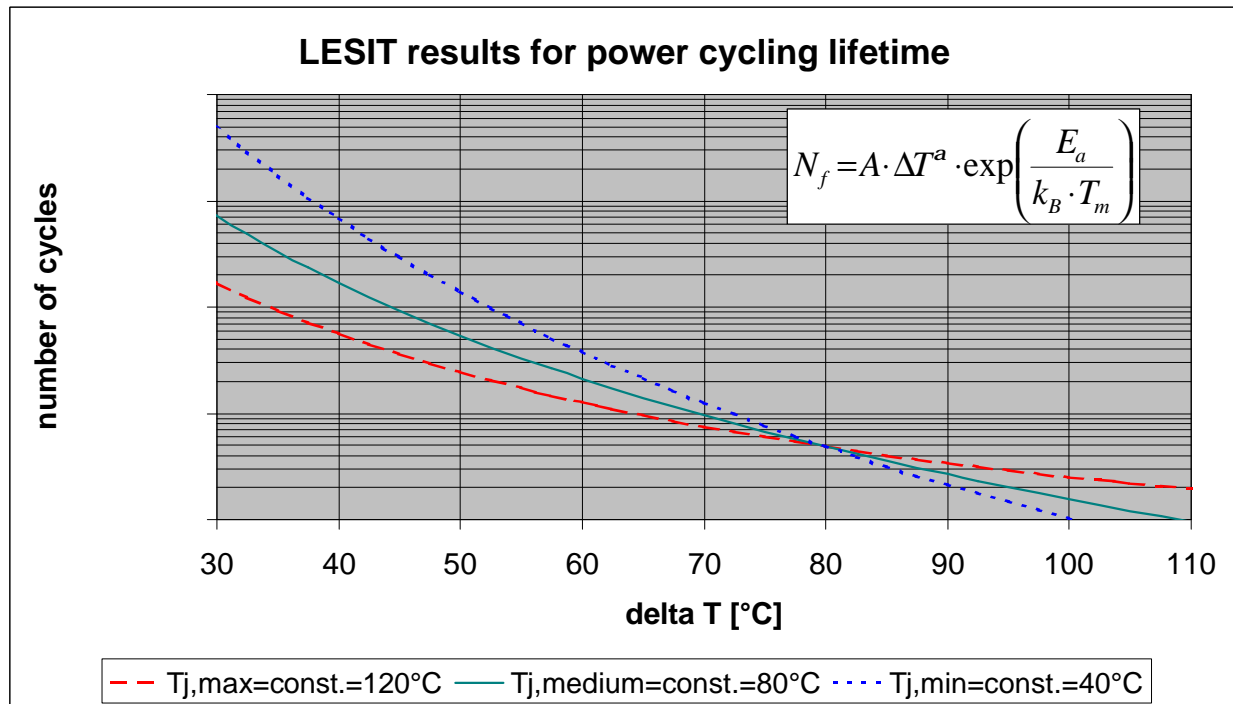


Figure 3.15 LESIT results for power cycling lifetime

3.3 Cooling of power modules

3.3.1 Cooling devices, coolants and cooling methods

The heat potential due to forward, switching and blocking losses in power modules has to be dissipated by means of heatsinks, which provide an expanded surface for convection and radiation, spreading the heat flow as well as reducing the intensity of transient thermal processes. Due to their isolation, all power modules of one system are mounted on to one common heatsink which may also serve as an element of the construction (case, chassis etc.).

Heat dissipation in a heatsink works on the principle that the heat is dissipated to the coolant either by direct heat transmission or via a heat carrier.

Heat carriers may be air, water or (more rarely) isolation oil, which is circulated by the effect of gravity or by fans or pumps.

Air in natural and forced motion or coolant mixtures on the basis of water may serve as coolants. In the following we would like to emphasise only natural (free convection) and forced air cooling and water cooling systems with one coolant circuit each, since more sophisticated cooling methods, such as “heatpipes” or boiling cooling are normally extremely application-specific and oil cooling is not very commonly used with power modules.

The heatsink material has to be constructed for optimal heat spreading (high heat transfer coefficient λ), with acceptable material and handling costs. Therefore, aluminum is often preferred ($\lambda = 247 \text{ W/K}\cdot\text{m}$ for pure Al), in special cases copper is also used ($\lambda = 398 \text{ W/K}\cdot\text{m}$). The dependence of heat spreading on the production process and the alloy used is remarkable; practical heatsinks show λ -values between $150 \text{ W/K}\cdot\text{m}$ (Al-die cast alloy) and $220 \text{ W/K}\cdot\text{m}$ (AlMgSi-extruded material).

Heat spreading has a considerable influence on the thermal efficiency of the heatsink. Therefore, optimized dimensioning of root thickness, number of fins, fin height and fin thickness is of importance:

- The *root* of a heatsink is the unfinned part of the mounting surface for the power modules, where the temperature gradient to the module base plate is relatively low and where the heat is spread.
- The *fins* of an air heatsink are used for dissipating the majority of the heat to the environment by radiation and convection. In water heatsinks this task is fulfilled by more or less structured *water channels*.

$$R_{\text{thha}} = \Delta T / P_{\text{tot}} = 1 / (\alpha \cdot A)$$

results from $Q = \alpha \cdot A \cdot \Delta T = P_{\text{tot}}$

(Q: dissipated heat quantity, α : heat transfer coefficient, A: heat transfer area, ΔT : temperature difference to the environment, P_{tot} : power dissipation, R_{thha} : heat transfer resistance of the heatsink)

It is recommended that a high number of fins is provided in order to increase the area of dissipation. But it has to be guaranteed that the flow conditions are set in a way which will not decrease α greatly.

Consequent to this conclusion, the different optimization criteria for heatsinks with natural and forced air cooling may be deducted.

The heatsink is heated more evenly when the power dissipation increases, i.e. the efficient heat exchange surfaces are enlarged; in Figure 3.16 the heat exchange surface is further extended by an increased heatsink length.

3.3.2 Thermal model of the cooling device

When explaining the thermal characteristics of power modules in chapter 1.4.2.2, the heatsink in the thermal equivalent block diagram had been described by only one “RC-element” (R_{thha} , Z_{thha}).

However, with an increase of power dissipation at $t = 0$ from $P = 0$ to $P = P_m$, the characteristic of the transient thermal impedance of the heatsink Z_{thha} versus time t is split up into several time constants as shown in Figure 3.16 with an example. The total thermal impedance characteristic $Z_{\text{thja}}(t)$ of the assembly may be determined by graphic addition of the thermal impedance characteristics of the power module and the heat transition to the heatsink.

The $Z_{\text{th}}(t)$ -curves may be plotted as the sum of v exponential functions using the following equations:

$$\Delta T(t) = P_m \cdot \sum_v R_{\text{thv}} [1 - \exp(-t/\tau_{\text{thv}})] \quad \text{and} \quad Z_{\text{thha}}(t) = \Delta T(t) / P_m$$